

## SIMPLIFIED ENVIRONMENTAL ANALYSIS OF THE LONG-TERM PERFORMANCE OF WOOD CLADDING AND DECKING

Jonas Niklewski<sup>1</sup>, Jakub Sandak<sup>2</sup>, Philip Bester van Niekerk<sup>3</sup>, Christian Brischke<sup>4</sup>, Richard Acquah<sup>2</sup>, Anna Sandak<sup>2</sup>

**ABSTRACT:** The performance of timber in exposed environments is affected by several biotic and abiotic factors. For timber cladding and decking, two important aspects include reduced structural performance due to fungal decay and aesthetical changes resulting from superficial effects such as photodegradation and moulds. Predicting the long-term performance of timber is important because it enables rational material (species and treatment) and design (detailing) choices and reduce the risks of unexpected repairs and premature replacement of timber products. In this paper, we use available data on material performance in conjunction with environmental analysis to model, in a simplified way, (1) the time until onset of fungal decay and (2) the long-term aesthetical appearance of timber facades and decking. The results demonstrate how the analysis can be used on a detailed geometry where wooden boards were modelled as separate objects and the choice of material affects the outcome. Several steps needing further development were identified, including a dose model linking microclimate to colour change and a better model for predicting moisture content. The study is part of a long-term effort to make holistic performance-based assessment of wood available for public use through easy-to-use procedures and accessible open-source software.

**KEYWORDS:** Wood, Aesthetics, Fungal decay, Durability, Long-term performance, Material database

### 1 INTRODUCTION

There are many different wood species, treatments, and material modifications available on the market. Selecting a material that meets a set of defined user criteria is far from trivial, in part because knowledge of long-term performance is fragmented or incomplete. The long-term performance of timber is affected by both biotic and abiotic mechanisms, and the time until non-performance depends on several aspects. In addition, the definition of non-performance depends on the application. For example, the main concern in the design of structural timber in outdoor applications, such as timber bridges, is generally the impaired structural performance caused by fungal decay. For other applications, such as cladding and decking, both structural integrity and long-term aesthetical performance/visual appearance are important aspects to consider.

Fungal decay leads to wood mass loss and reduced structural integrity, with wood moisture content being one of the main vectors for material deterioration. Free water is a prerequisite for the degradation process, so attack by decay fungi is usually not seen as a risk when the wood moisture content is below cell-wall saturation or when the wood temperature is below freezing [1]. Wood in outdoor exposure is also subject to superficial damage and colour

changes not directly associated with structural damage. Colour change is caused by both chemical changes and biological growth. Solar irradiance and wind-driven rain have been cited as the most influential factors driving colour change [2]. Surfaces exposed to UV and visible light will develop a cellulose-rich grayish surface layer, in part due to the decomposition and leaching of lignin [3].

While these two modes of material deterioration lead to different outcomes and consequences, both can be described as functions of material characteristics and environmental exposures. Figure 1 shows, conceptually, a model for deterioration caused by environmental effects. The material database describes how the material (species and modification/ treatment) in question responds to environmental exposure. The environmental exposure can be modelled from the local weather and the geometry of the building envelope. The dose model evaluates these exposures (e.g. rain, temperature) and converts them to a unitless measure of dose. If other input variables are required, such as as moisture content and surface temperature, then those are derived from environmental exposures prior to dose modelling. The exposure dose can then be compared against the resistance to infer the material's response.

<sup>1</sup> Jonas Niklewski, Lund University, Department of Building and Environmental Technology, Sweden, jonas.niklewski@kstr.lth.se

<sup>2</sup> Jakub Sandak, Anna Sandak, Richard Acquah, InnoRenew CoE, Slovenia / University of Primorska, Slovenia, jakub.sandak@innorenew.eu

<sup>3</sup> Philip Bester van Niekerk, University of Goettingen, Wood Biology and Wood Products, Germany, philipbester.niekerk@uni-goettingen.de

<sup>4</sup> Christian Brischke, Thuenen-Institute of Wood Research, Hamburg, Germany, christian.brischke@thuenen.de

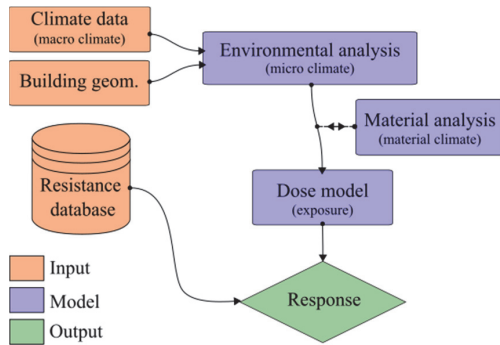


**Figure 1:** Conceptual illustration of the models linking the material database to environmental exposures.

Dose modelling has previously been used as a basis for factorised guidelines targeting service life of wood in above-ground applications [4]. Here, a ‘factor’ is a unitless measure describing the relative change in service life of a reference case stemming from, for example, a variation in climate conditions or design detailing. Dose models allow factors to be derived from moisture- and temperature conditions, which can be measured or simulated. Factorisation generally relies on simplified interaction between exposures, meaning that synergistic or antagonistic effects are not adequately accounted for. To address this problem, some efforts have been made to limit the use of factorisation by instead expanding the scope of moisture modelling [5]. This study is a continuation of this work, targeting wind-driven rain and shelter through environmental analysis.

Environmental conditions affect the performance of the building envelope. Exposure to wind-driven rain (WDR) and sunlight both vary with orientation and surface tilt, but also depend on design detailing. For example, deep roof eaves have long been used to limit the exposure of WDR on walls. Solar radiation is relatively predictable and can be modelled by ray-tracing. WDR is more chaotic, but can be modelled by computational fluid dynamics (CFD) [6]. As a simpler alternative to the computationally heavy CFD analysis, WDR can also be modelled through ray-tracing [7]. A simple method for environmental analysis of buildings using ray-tracing has previously been proposed by Charisi et al. [8], including both WDR and solar radiation.

The focus of the present paper is to demonstrate how (simplified) environmental analysis combines with other models to link environmental exposures to existing material databases for fungal decay and photodeterioration. WDR and solar radiation were modelled in Blender 3D [9] through particle- and ray-tracing, respectively. The resulting exposures were used as input to calculate moisture content and combined fungal dose. A basic fuzzy inference system (FIS) was used to create semi-realistic colour changes from exposure to WDR and solar radiation. While the FIS model assumptions are subjective, the system can easily

be tuned when additional validation data becomes available. The analysis as a whole is simple, relatively fast and relies entirely on OA software to ensure high accessibility.

## 2 METHODS

This section describes the models involved in predicting aesthetical and decay performance of wooden cladding and decking. The nature of the models involved differs depending on the deteriorating mechanism in question. In both cases, the analysis is based on a specific 3D geometry of the building and the local climate. Climate data were obtained from the Swedish Meteorological and Hydrological Institute (SMHI), measured in Gothenburg, Sweden, between 1<sup>st</sup> of January and 31<sup>st</sup> of December in 2021.

### 2.1 MATERIAL DATABASE

Material data for the relative resistance to fungal decay of treated, modified and natural wood species were obtained from Brischke et al. [10]. The data are based on a meta-analysis of measured data on moisture dynamics and inherent resistance. These measurements were used with the Meyer-Veltrup resistance model [11] to estimate the resistance to fungal attack in above-ground applications.

Material data for the colour change of modified and treated wood species were obtained from Sandak et al. [12]. The data set is based on a test-setup where the colour of different wood products was recorded monthly during 24 months of outdoor exposure. The database describes how the late- and earlywood colours vary over time. While a dose model for linking the colour change to weather variables has not yet been developed, the material data alone can be used in conjunction with a simplified exposure criterion to predict the final visual appearance of wood cladding and decking.

### 2.2 ENVIRONMENTAL ANALYSIS

The environmental analysis is performed in Blender 3D (v.2.83.20.0), an open-source 3D-modelling environment with limited physics-based simulation and analysis capabilities. Since Blender is not a dedicated numerical software, some simplifications are necessary. It should be noted, however, that the functionality to use the software for more sophisticated environment analysis, even CFD, is possible by integration of other open-source software [13].

The 3D geometry of a smaller playhouse (see Figure 2) is used here to demonstrate the concept. The model was obtained from a third party, meaning that the geometry was not tailored to simplify the analysis. The cladding is designed with vertical boards (125x20 mm<sup>2</sup>) and battens (45x20 mm<sup>2</sup>), i.e. vertical boards in two planes. Each board is modelled as a separate object, with eight vertices and six faces. The geometry was never remodelled or manipulated to facilitate the analysis.

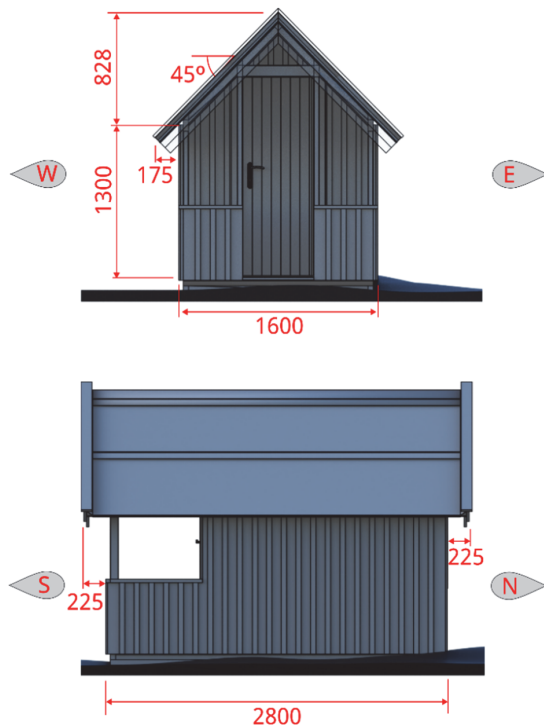


**Figure 2:** Object geometry and dimensions. The annotated arrows (E and N) indicate orientation.

After importing the geometry to Blender 3D, wooden objects to be included in the environmental analysis are inspected to verify that surface normals are consistent with respect to their orientation. The object surfaces are then projected onto a combined flat surface (UV map), using a method to maintain consistent scale between objects. The UV map is a flat representation of object surfaces linking vertex coordinates (xyz) to texture coordinates (uv). This map is used here to store the results from the environmental analysis, such as WDR and solar radiation. With a resolution of 1024x1024, a single pixel represents an area of about 10x10 mm<sup>2</sup>, meaning that the width of a board (125 mm) is about 13 px with a thickness (20 mm) of 2 px. A single pixel is hereafter referred to as a node.

The methodology for calculating WDR and direct radiation follows the same principle. Both effects are assumed to follow straight trajectories. The trajectory of direct beam radiation depends on the sun's position, and that of precipitation depends on the wind speed, wind direction and terminal velocity. Following the assumption of straight trajectories, hourly solar radiation and WDR obtained from climate data were projected onto the surface normals of the geometry. In a subsequent step, binary masks were used to filter out exposure in shaded or sheltered regions of the geometry. The binary masks were obtained through different methods depending on the exposure in question, as explained in the following sections.

### 2.2.1 Exposure to wind-driven rain

The protocol for simplified environmental analysis of WDR presented here builds on a set of software-specific features, including animations, particle physics, 'dynamic paint' and 'texture baking'.

WDR is modelled as a particle system using the Blender physics engine. A particle system has two components: an emitter plane and particles. Particles are emitted from the emitter plane with an initial velocity and follows trajectory based on predefined physics, see Figure 3. The particle behaviour on collision with other objects can be set to, for example, disappearing, sticking or bouncing off the surface with or without damping. Here, particles are set to drop all momentum on collision and then continue in the direction of gravity, thus emulating water runoff.

The feature 'dynamic paint' is used to map particle collisions to the geometry. In general, dynamic paint is used to modify a surface (canvas) based on its proximity to another object (brush). Here, the particle system was defined as brush and the wooden objects (cladding/deck) were defined as canvas. The canvas was set to change colour from white to black (binary) on direct contact with a particle. The radius of brush (particle) on contact was set to 10 mm. The radius of the resulting patch was set to expand to a final radius of about 40 mm. The latter ensured that regions near the point of particle collision were also categorised as exposed.

A square horizontal emitter plane (8x8 m<sup>2</sup>) was defined approximately 1 m above the geometry. The plane was set to emit particles in a uniform grid with a resolution of 250x250, which for the given geometry resulted in sufficient detail. The initial vertical velocity ( $v_z$ ) of the particles was set to 4.5 m/s. This value is commonly used as the terminal velocity of raindrops with a drop diameter of 1.2 mm and can be used for light to moderate intensity rain spells [6]. The horizontal velocity ( $v_x, v_y$ ) was varied to simulate different wind speeds and directions. Wind directions and speeds were modelled between 0 and 315 degrees in increments of 45 degrees and 0 to 6 m/s in increments of 1 m/s, respectively, resulting in 49 different unique scenarios. Note that  $v=0$  m/s is was not run for varying orientations. The simulations were run programmatically in batch using the Blender API for Python. The outcome of the analysis resulted in 49 binary masks describing the exposed regions for each scenario of precipitation.

The terminal velocity of rain-drops combined with the wind direction and velocity gives the trajectory,  $\mathbf{R}$ . The projection of  $\mathbf{R}$  on the surface (unit) normal of each node  $\hat{\mathbf{n}}_{uv}$  is given by the dot-product. The magnitude of this vector divided by the terminal velocity gives the ratio of WDR in the node relative to rain passing through a fictive horizontal plane, which is also known as the wall factor. The wall factor is a convenient metric which can be multiplied by precipitation measured through a horizontal

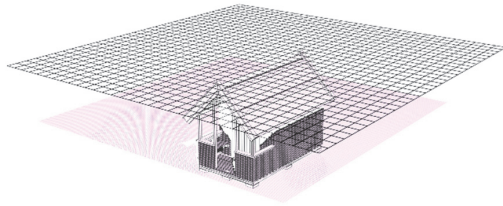


**Figure 3:** Particle system simulating rain from a southeast orientation. The corresponding binary exposure map is projected on the cladding/deck, where white colour indicate sheltered areas.

plane to calculate the amount of rain on a surface with arbitrary orientation and inclination. The binary maps obtained in the previous step were then used to zero out any nodes which were sheltered from rain. For each hour, the binary map corresponding to the nearest velocity (wind speed) and orientation was used.

### 2.2.2 Exposure to solar irradiance

Solar irradiation is limited to direct (beam) and diffuse irradiation. Here, the effect of reflected irradiance is not considered. Similar to the analysis of WDR, the calculation of solar irradiation on surfaces with different shading, tilt and orientation is performed in two steps. In a first step, the exposed regions of the geometry are identified using ray-tracing. In the second step, the irradiation incident on each node is calculated by projection onto the surface normals.

Regions shaded from direct solar irradiation were identified using the built-in ray-tracing algorithm of the 'cycles' renderer, a 'sun' light source and the built-in sun path algorithm. In Blender, the 'sun' is a directional light source with constant intensity, meaning that the scene lighting depends only on a given angle. This angle is given by the position of the sun in the sky relative to the location of the building, i.e. the azimuth,  $\alpha$ , and altitude,  $\beta$ . The position of the sun is a function of geographical coordinates and time. For each hour, the shadow caused by the sun is mapped, resulting in 8760 binary images.

The hourly direct irradiation in each node was calculated from the direct normal irradiance,  $I_d$ , measured via satellite by SMHI [14]. The azimuth and elevation angles translate to a unit vector,  $\hat{n}_{I_d}$ , which multiplied by scalar  $I_d$  gives the vector,  $\mathbf{I}_d$ . The procedure is then analogous to the one presented in section 2.2.1, but the vector  $\mathbf{R}$  is substituted by  $\mathbf{I}_d$ . For each hour, the direct beam irradiance normal to each surface was calculated by the projection of  $\mathbf{I}_d$  on the surface normal of each node  $\hat{n}_{uv}$ . The corresponding shadowmap, as described in the previous paragraph, was then used to zero out any shaded nodes on the geometry.

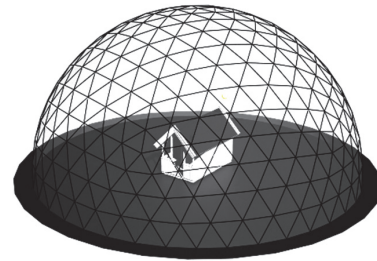


**Figure 4:** Skydome used to estimate the sky view factor.

Diffuse isotropic irradiation was modelled using the sky view factor (SVF). The SVF is a dimensionless value describing the proportion of visible sky from a node. The SVF depends on surface tilt and obstacles. For example, the SVF of a vertical wall facing a free horizon is 0.5. The diffuse irradiation incident on any node on the geometry can be calculated by multiplying the measured diffuse radiation by the corresponding SVF.

The SVF was calculated by modelling the atmosphere as a dome discretised into 600 triangular sky patches having equal area, see Figure 4. The surface normal of each sky patch was used to set the direction of a sun light source. The built-in ray-tracing algorithm was then used to map the visible part of the geometry from each sky patch. For this part of the geometry, the incident irradiation in every node was calculated. Finally, the sum total irradiation in every node were divided by that of a horizontal unobstructed surface, to obtain the SVF.

## 2.3 DECAY PERFORMANCE

The development of fungal decay over time is a function of the material climate (moisture content and temperature) and the material resistance (presence of extractives, treatment, etc.) to decay. The material climate depends on the environmental conditions (exposure) but is also inherently dependent on the moisture dynamics (permeability) of the wood product. For a simplified analysis following the structure in Figure 1, the exposure dose is modelled as material independent, and the moisture performance is instead considered as part of the material resistance.

### 2.3.1 Moisture performance

The moisture content is estimated from daily averages of relative humidity and temperature and daily sums of precipitation using an existing model developed by Frühwald et al. [15]. The equilibrium moisture content,  $u$ , is here calculated as follows:

$$u(\phi) = 0.7\phi^3 - 0.8\phi^2 + 0.42\phi + 0.0077 \quad (1)$$

where  $\phi$  is the daily average relative humidity. The daily average moisture content of a fictive sheltered board,  $u_{01}$ , is calculated from the average equilibrium moisture content over two consecutive days. During rainy periods, the actual moisture content of a board will increase and temporarily exceed that of the sheltered board. In the

model, a rainy day is defined by the daily sum of precipitation exceeding 4 mm, and a rainy period,  $t_r$ , is defined by the number of consecutive days when this condition is met. The moisture content during rainy periods,  $u_1$ , is then described as:

$$u_1(t_i) = u_{01}(t_i)[1 + k_r] \quad (2)$$

where  $k_r$  depends on the wood species and duration of the rain event. Here, a value of  $k_r=0.8$  was used, as proposed by Frühwald et al. [15]. When the rainy period ends, the moisture content,  $u_1$ , will decrease towards the moisture content of the sheltered board,  $u_{01}$ . The duration of this decrease,  $t_d$ , depends on the length of the previous rainy period (number of consecutive days with rain), and is described as  $t_d=2.5t_r$ . The moisture content  $k$  days after a rainy period can then be calculated as:

$$u_1(t) = \max\left(\frac{k(u_{01}k_r)/t_d}{u_{01}}\right) \quad (3)$$

The exposure to precipitation [mm/day] depends on the surface normal (orientation and inclination) and the degree of sheltering. Every node in the geometry is associated with a time-series of precipitation, obtained from the environmental analysis. Relative humidity and temperature were obtained from the weather data and were assumed uniform over the building geometry. In practice, solar irradiance will affect the temperature and relative humidity of the wood surface.

### 2.3.2 Dose model

In this paper, the 'logistic' dose model from [16] was used to estimate the progression of decay from the moisture- and temperature variation. The model is comprised of two functions: the moisture-induced dose,  $D_u(u)$ , and the temperature-induced dose,  $D_T(T)$ , as shown in Figure 5. The dose is a dimensionless value which describes the development of fungal decay between unfavourable (0) and ideal (1) conditions. The functions are mechanistic in the sense that their cardinal points (minimum, maximum, optimum) are based on mycology research [1]. If either  $D_T$  or  $D_u$  is zero, then it is assumed that no decay development can occur on that day. If both terms are positive, then the daily dose is calculated as a weighted average of the two components, according to:

$$D = \frac{3.2D_T + D_u}{4.2} \quad (4)$$

The dose,  $D$ , accumulates over time, with no setback, and relates directly to the decay rating. The relationship between decay rating and dose is based on long-term field trials where the moisture content, temperature and decay rating of Scots pine sapwood (*Pinus sylvestris*) and Douglas-fir heartwood (*Pseudotsuga menziesii*) were monitored [17]. It was found that decay rating 1 corresponds to a dose of approximately  $D=325$ , meaning that the species used in the test sustain about 325 days in ideal conditions (for fungal decay) prior to the initiation of fungal decay [18].

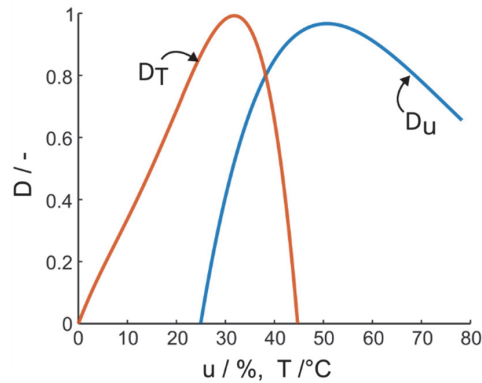


Figure 5: Dose functions describing the relative temperature- and moisture conditions for fungal decay.

The limit state is herein defined as the time until the onset of decay. The time until the limit state is reached is calculated as the ratio  $D_{Rd}/D_{Ed}$ , where  $D_{Rd}$  is the resistance dose obtained from the material database based on [10].

### 2.3.3 Factorisation

Due to its simplicity, the factorised approach has been commonly used for design guidelines. Here, the annual exposure dose,  $D_{Ed}$ , is calculated as follows:

$$D_{Ed} = D_0 k_1 k_2 k_3 \quad (5)$$

where  $D_0$  is a reference value depending on the ambient climate and  $k_1$ ,  $k_2$  and  $k_3$  are factors to account for moisture trapping, sheltering and distance to ground, respectively. Other factors can also be included.

In this paper, the dose derived from the environmental analysis explicitly considers ambient conditions,  $D_0$ , and sheltering,  $k_2$ , in the process of modelling moisture content variation. Distance to ground is considered in analogy with the factor-based method by calculating the distance in every node to a ground plane and then using the relationship in [19] to calculate the relative increase in dose:

$$k_3 = \begin{cases} \frac{700 - a}{300} & a < 400 \\ 1.0 & a \geq 400 \end{cases} \quad (6)$$

The distance in every node was here obtained through dynamic paint by defining the ground plane as a brush and the wooden elements collectively as canvas. Each node on the canvas was then coloured based on proximity to the brush with a linear falling intensity from direct contact with the ground (1) to a distance exceeding 400 mm (0).

## 2.4 AESTHETICAL PERFORMANCE

The change in visual appearance is modelled by combining a map of exposure dose and a generic procedural wood texture with the colour database from [12]. A fully functional dose model linking microclimate to colour change does not yet exist. Instead, conditional

statements and fuzzy logic were used to create pseudorealistic weathering patterns.

Colour change caused by photodegradation requires solar radiation to break down the wood cell structure and water to wash off the by-products [20,21]. Whether or not a surface is subject to weathering can thus be inferred from a conditional statement. It can further be assumed that, given a sufficiently long time horizon, surfaces exposed to both solar irradiance and WDR converge to a fully weathered state. This logic is useful for binary classification but is unable to reproduce the characteristic gradual weathering patterns between weathered and non-weathered regions. Here, a multivalued conditional approach based on (fuzzy) logic was used to define a function for interpolating between the two extremes. To demonstrate the concept, a set of subjective assumptions was made.

The function describing the degree of weathering depends on two crisp (numeric) input variables: solar radiation and precipitation. To make use of fuzzy logic, these input variables were fuzzified into two linguistic terms: low, and high exposure. Similarly, the output was described as low and high degree of weathering. The following rules were defined:

1.  $D == \text{low} \parallel R == \text{low} \rightarrow W = \text{low}$
2.  $D \sim= \text{low} \& R \sim= \text{low} \rightarrow W = \text{high}$

The first rule states that both precipitation and solar radiation may limit the rate of degradation, i.e. if either of the two is zero, then no degradation will occur. The second rule simply describes that if (1) is false, then the degree of weathering is high. Membership functions and the resulting response surface are shown in Figure 6. The membership functions were, for simplicity, assumed triangular with their centre of gravity at 0 and 1, respectively. The resulting response surface shows that no weathering occurs if the node is subject to less than about 5% of the maximum precipitation or solar irradiance, respectively. The shape of the interpolated region between 5% and 10% is determined by the shape of the input membership functions.

The node colour is determined from wood texture and the degree of weathering using colour data from the database. The FIS determines the degree of weathering in each node and the resulting distribution is hereafter referred to as the 'dose map'. In addition to the degree of weathering, the colour depends on whether the node is late- or earlywood, which is determined from the material texture. Here, a procedural wood texture is used where the intensity describes the wood type, i.e. white (1) being earlywood and black (0) being latewood. A value between 0 and 1 describes a mix of latewood and earlywood where the colour is interpolated.

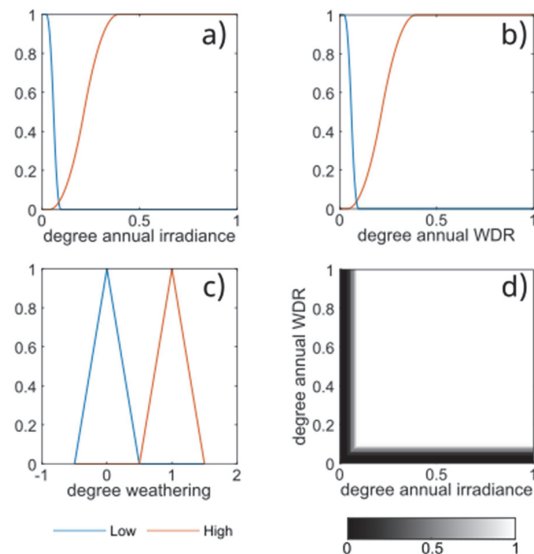


**Figure 6:** Input membership functions (a,b), output membership functions (c) and response surface (d).

## 3 RESULTS AND DISCUSSION

### 3.1 ENVIRONMENTAL ANALYSIS

Figure 7 shows the sky view factor (SVF) of the geometry, the total irradiance (direct + diffuse) and the annual exposure to wind-driven rain. The SVF shows that isotropic diffuse radiation is not orientation-dependent, but depends on the degree of sheltering and surface tilt. Therefore, horizontal surfaces on the cladding absorb approximately the same amount of diffuse radiation. The vague light vertical lines on the façade is a result of the design of the cladding, where the outer layer (battens) partially shades the inner layer (boards).

Exposure to solar radiation is higher in the southern orientation, which is typical for buildings in the northern hemisphere. The southern cladding is also subject to more WDR than the other vertical faces, which is typical for Sweden. The maximum WDR (500-600 mm) can be observed on the horizontal boards of the deck. Vertical surfaces close to the ground facing south, west, east and north were subject to approximately 300, 150, 150 and 100 mm of WDR, respectively. These values are consistent with values calculated without considering any sheltering effects.

The environmental analysis was performed for a given time, site, and geometry. However, redoing the entire analysis is necessary only when the geometry is changed. This is an advantage stemming from the fact that weather data was not integrated directly with ray-tracing and particle simulations. Particle simulations were performed based on generic scenarios and are therefore independent of both time-period and location. Ray-tracing on the other hand depends on geometry, location and time-period. The effect of calendar year on the sun position is for practical

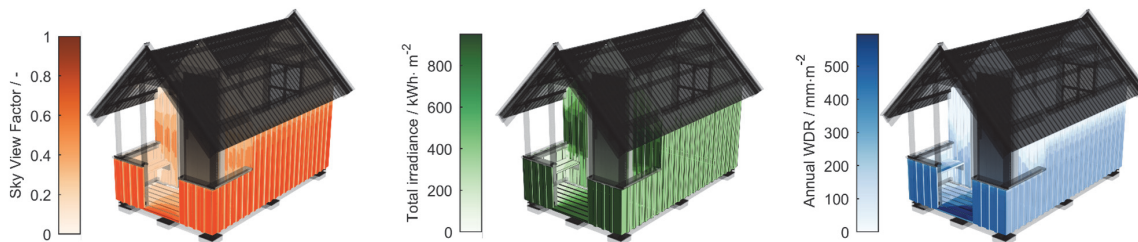


**Figure 7:** Sky view factor (a), total solar irradiance (b) and annual wind-driven rain (c), viewed from southeast.

purposes negligible, so the analysis can be reused for different years. Similarly, location can be varied within reasonable limits without introducing major errors stemming from variations in sun position. Alternatively, ray-tracing could be made independent of time-period and location by using generic scenarios of sun position. The analysis of sky view factor is only dependent on the geometry.

### 3.2 Fungal decay

Figure 8 shows the variation of exposure dose. The dose values range between 1 and 50, depending on orientation, tilt, degree of shelter and distance to the ground. The highest dose values are found close to the ground on the horizontal decking boards, while values close to zero are found on interior surfaces and other locations completely protected from rain, e.g. below the roof eaves. The high dose values seen on the decking boards can be explained by them being exposed to WDR from the most severe (south) orientation in conjunction with unfavorable surface normals (horizontal boards) and small distance to the ground.

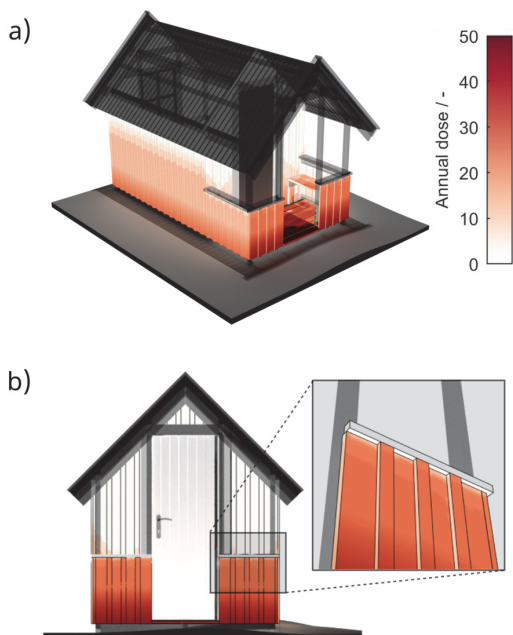


**Figure 8:** Distribution of fungal dose viewed from southwest (top) and south (bottom).

Fully sheltered elements categorised in use class 2 [22] would, under normal circumstances, not be expected to decay. Yet, the results indicate a non-zero dose also for surfaces completely sheltered from WDR. This can be explained by the moisture model employed, specifically equation 2 exceeding the lower threshold for fungal decay (25%) when the relative humidity exceeds 90%. However, the dose values registered on surfaces sheltered from WDR are very small relative to the values on exposed surfaces, and therefore have little or no influence on the service life of the building as a whole.

It should be noted that the dose shown Figure 8 does neither account for detailing nor for end-grain absorption. Therefore, the depicted dose should be regarded as a reference value to be multiplied by factor  $k_3$  in regions affected by moisture trapping or exposed end-grain. For example, Figure 8b shows a southern view with a set of vertical exposed boards connected to a horizontal member. The vertical boards are subject to a dose of approximately 20 in the connection to the horizontal board. If the end-grain is directly exposed to precipitation and no ventilated gap (minimum 5-8 mm to facilitate drying) is provided, then the dose will increase by a factor of  $k_3=1.6$  up to 32, following the guideline by Isaksson et al. [19].

The dose shown in Figure 8 is only dependent on the exposure conditions and is thus independent of the wood species, treatment and modification used. The actual service life depends to a great extent on the moisture-performance and inherent resistance of the wood product. These factors are considered by the material resistance dose, which is listed [10] for many different wood products. For example, untreated Norway spruce (*Picea abies*) and European larch (*Larix decidua*) have material resistances in above-ground applications of  $D_{Rd}=325$  and  $D_{Rd}=1800$ , respectively.

### 3.3 AESTHETICAL PERFORMANCE

Figure 9 shows the change in colour from newly built to weathered, with materials including natural and treated pine wood. The wooden materials were rendered without passing the materials through a shader. This means that interaction between material and lightning was not modelled. For demonstrative purposes this was deemed desirable.

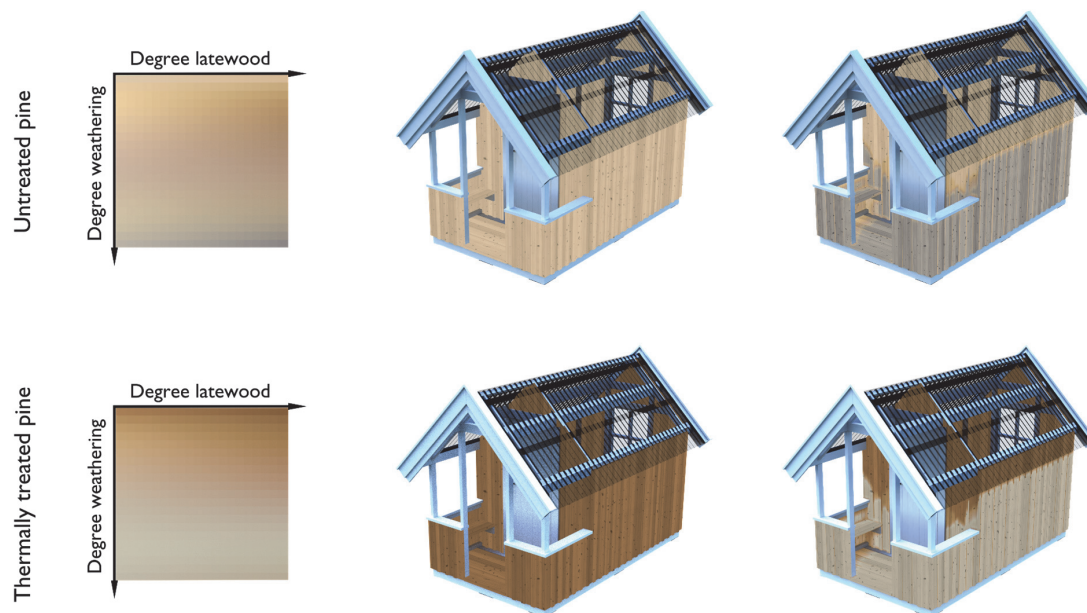


**Figure 9:** Colour of newly built (centre column) and fully weathered building (right column) made from natural (top row) and thermally modified (bottom row) pine wood, viewed from southeast. The left column shows the interpolated colour maps, based on the database.

As can be seen by comparison to Figure 7, the extent of the weathered regions correspond quite well with the coverage of WDR. The reason for this is that the FIS require both exposure to precipitation and solar irradiance for weathering to occur. Regions exposed to WDR are predominantly exposed also to direct and/or diffuse radiation, thus making exposure to precipitation the limiting factor.

It should be reiterated that the FIS model used to determine the dose map is very simplified and is used in lieu of an accurate dose model. The approach presented here can be used for binary classification of regions subjected or not subjected to weathering and for smooth interpolation between those regions. However, the model cannot be used to describe the kinetics of weathering, i.e. the aesthetical appearance at a specific point in time.

#### 4 CONCLUSIONS

Exposures to WDR and solar radiation were modelled on a multi-object geometry. Ray-tracing for solar radiation and particle tracing for WDR were performed in the open-source software Blender 3D. The results were then used to model exposure to fungal decay and to identify areas subject to surface deterioration, respectively. These results, in conjunction with existing material databases, can be used as a basis for service life prediction.

The methods demonstrated here can be used to support decision-makers in the choice of material and design. The results provide a visual overview which can be used to qualitatively identify critical locations where detailing should be designed with caution, as well as regions where

detailing is less important. Based on the results, the designer can decide whether the long-term performance, in terms of service life and aesthetics, is acceptable. If not, then the design can easily be adapted with material less prone to weathering and/or with higher resistance to fungal decay.

Future work will focus on improving the model used to estimate moisture content and developing a quantitative dose-response model relating colour change to environmental effects. The scope of the moisture content calculation could also be expanded to include distance to ground and detailing, further reducing the need for factorised design. Finally, the method can be integrated with life cycle costing and maintenance scheduling, as it provides detailed information of exposure for individual components. However, model validation against real examples is needed.

#### ACKNOWLEDGEMENT

Authors received funding in the frame of the research projects *CLICKdesign* and *WoodLCC*, both supported under the umbrella of ERA-NET Cofund *ForestValue* through the national funders of the participating countries. *ForestValue* has received funding from the European Union's Horizon2020 research and innovation programme under GA N° 773324. JS, RA and AS gratefully acknowledge the European Commission for funding the *InnoRenew CoE* project (GA #739574) under the Horizon2020 Widespread-Teaming program and the Republic of Slovenia (investment funding from the Republic of Slovenia and the European Regional Development Fund).

## REFERENCES

- [1] Schmidt O.: Wood and tree fungi, Springer, 2006.
- [2] Rütther P., Jelle B.P.: Color changes of wood and wood-based materials due to natural and artificial weathering. *Wood Material Science & Engineering*, 8:13–25, 2013.
- [3] Kalnins M.A., Feist W.C.: Increase in wettability of wood with weathering. *Forest Products Journal*, 43(2):55–57, 1993.
- [4] Thelandersson S., Isaksson T., Frühwald E., Toratti T., Viitanen H., Grüll G., Jermer J., Suttie E.: Service life of wood in outdoor above ground applications: Engineering design guideline. Lund University, Lund, 2011.
- [5] Niklewski J., Van Niekerk P.B., Brischke C., Frühwald Hansson E.: Evaluation of moisture and decay models for a new design framework for decay prediction of wood. *Forests*, 12:721, 2021.
- [6] Blocken B., Carmeliet J.: Validation of CFD simulations of wind-driven rain on a low-rise building façade. *Building and Environment*, 42:2530–2548, 2007.
- [7] Tsoka S., Thiis T.K.: Calculation of the driving rain wall factor using ray tracing. *Journal of Wind Engineering and Industrial Aerodynamics*, 179:190–199, 2018.
- [8] Charisi S., Thiis T.K., Stefansson P., Burud I.: Prediction model of microclimatic surface conditions on building façades. *Building and Environment*, 128: 46–54, 2018.
- [9] Blender Online Community: Blender - a 3D modelling and rendering package. Blender Foundation, Blender Institute, Amsterdam, <http://www.blender.org>, 2022.
- [10] Brischke C., Alfredsen G., Humar M., Conti E., Cookson L., Emmerich L., Flæte P.O., Fortino S., Francis L., Hundhausen U., et al: Modelling the material resistance of wood—Part 3: Relative resistance in above-and in-ground situations—Results of a global survey. *Forests*, 12(5): 590, 2021.
- [11] Brischke C., Alfredsen G., Humar M., Conti E., Cookson L., Emmerich L., Flæte P.O., Fortino S., Francis L., Hundhausen U., et al.: Modelling the material resistance of wood—Part 2: Validation and Optimization of the Meyer-Veltrup Model. *Forests*, 12(5):576, 2021.
- [12] Sandak A., Sandak J., Brzezicki M., Kutnar A.: Bio-based building skin. Springer Nature, 2019.
- [13] Southall R., Biljecki F.: The VI-Suite: a set of environmental analysis tools with geospatial data applications. *Open Geospatial Data, Software and Standards*, 2: 1–13, 2017.
- [14] Swedish Meteorological and Hydrological Institute, (n.d.). [www.strang.smhi.se](http://www.strang.smhi.se) (accessed January 12, 2023).
- [15] Frühwald Hansson E., Brischke C., Meyer L., Isaksson T., Thelandersson S., Kavurmaci D.: Durability of timber outdoor structures: modelling performance and climate impacts. In: *Proceedings of the World Conference on Timber Engineering 2012 (WCTE 2012)*, Auckland, New Zealand, 2012.
- [16] Isaksson T., Brischke C., Thelandersson S.: Development of decay performance models for outdoor timber structures. *Materials and Structures*, 46: 1209–1225, 2013.
- [17] Brischke C., Rapp A.O.: Dose–response relationships between wood moisture content, wood temperature and fungal decay determined for 23 European field test sites. *Wood Science and Technology*, 42: 507–518, 2008.
- [18] Alfredsen G., Brischke C., Marais B.N., Stein R.F., Zimmer K., Humar M.: Modelling the material resistance of wood—Part 1: Utilizing durability test data based on different reference wood species. *Forests*, 12(5):558, 2021.
- [19] Isaksson T., Thelandersson S., Jermer J., Brischke C.: Beständighet för utomhusträ ovan mark (in English: service life of wood above ground). Structural Engineering, Lund, 2011.
- [20] Derbyshire H., Miller E.R.: The photodegradation of wood during solar irradiation. *Holz Als Roh-Und Werkstoff*, 39: 341–350, 1981.
- [21] George B., Suttie E., Merlin A., Deglise X.: Photodegradation and photostabilisation of wood—the state of the art. *Polymer Degradation and Stability*, 88(2):268–274, 2005.
- [22] EN 335: Durability of wood and wood-based products - Use classes: definition, application to solid wood and wood-based products, 2013.